Bernardo *et al. Int J Concr Struct Mater (2018) 12:62*
https://doi.org/10.1186/s40069-018-0285-0

International Journal of Concrete Structures and Materials

ORIGINAL ARTICLE

Open Access

Generalized Softened Variable Angle Truss Model for PC Beams under Torsion

Luís F. A. Bernardo[1*], Cátia S. B. Taborda[2] and Jorge M. A. Andrade[2]

Abstract

In a previous study, a new model (Generalized Softened Variable Angle Truss Model—GSVATM) was proposed to compute the global behavior of reinforced concrete beams under torsion, including for low loading stages. In this article, the GSVATM is extended to cover prestressed concrete (PC) beams under torsion, with longitudinal and uniform prestress. The changes in the GSVATM, in order to include the influence of the initial stress state due to prestress, the contribution of the prestress reinforcement after the decompression of concrete and the constitutive laws for prestress reinforcement, are presented, as well as the solution procedure. The theoretical predictions of the extended GSVATM are compared with experimental results of PC beams under torsion, where good agreement is observed in terms of stiffness, transition from the non-cracked stage to the cracked stage and also in terms of the maximum torque. It is also shown that when compared with the predictions of some codes of practice, namely for the cracking and ultimate torque, the estimates from the GSVATM are in general more accurate.

Keywords: prestressed concrete, beams, torsion, GSVATM

1 Background

Since the last century, the Space Truss Analogy (STA) has been one of the most comprehensive and used analytical tools to model the behavior of reinforced concrete (RC) beams under torsion. Nowadays, it constitutes the basis of several codes of practice, namely the American Code (since 1995) and the European Model Code (since 1978).

Since its first version proposed in the beginning of the last century, the STA for RC beams under torsion has undergone several developments, mainly in the last three decades. For the sake of this article, some of the recent developments are referred below.

Based on previous developments of the STA, namely the incorporation of a variable angle for the direction of the principal compressive stresses for concrete, Hsu and Mo (1985a, b) proposed the Variable Angle Truss Model (VATM). This model aimed to unify the torsional design of beams with small and large cross sections, as well as RC beams and beams with longitudinal and uniform prestress, that is, prestressed concrete (PC) beams. In the VATM, the conventional stress (σ)–strain (ε) relationship for uniaxial compressive concrete was substituted by a smeared softened σ–ε relationship to account for the softening effect (influence of the diagonal cracks due to the perpendicular tensile stresses). VATM proved to give good results for the ultimate torsional behavior of RC and PC beams (Hsu and Mo 1985a, b). This is because VATM neglects the concrete tensile strength and also the influence of the concrete core for plain beams, so this model approaches the real model only for high loading stages (Hsu and Mo 1985a, b; Bernardo et al. 2012a). Further studies also shown that the σ–ε relationships used to simulate the behavior of the materials constitute also a very important factor for VATM to be able to provide accurate predictions for high loading stages, both for RC and PC beams under torsion (Bernardo et al. 2012a; Bernardo and Andrade 2017).

In general, the VATM provides a simple physical understanding of the torsional behavior of structural concrete beams after cracking. For this reason, since 1985 refined versions of the VATM have been proposed for RC and PC beams under pure torsion (Rahal and Collins 1996; Bhatti and Almughrabi 1996; Wang and Hsu

*Correspondence: lfb@ubi.pt
[1] C-MADE—Centre of Materials and Building Technologies, University of Beira Interior, Covilhã, Portugal
Full list of author information is available at the end of the article
Journal information: ISSN 1976-0485 / eISSN 2234-1315

1997), for RC beams under torsion combined with other internal forces (Silva et al. 2017; Greene and Belarbi 2009; Rahal and Collins 2003; Taborda 2017) and also for RC beams under torsion with axial restriction (Bernardo et al. 2015a, b). Additional and more advanced analytical models, not directly based on the STA, have also been proposed in previous studies, including for beams under combined loading with torsion, for instance (Alnauimi and Bhatt 2004; Bairan Garcia and Mari Bernat 2007; Karayannis 2000; Karayannis and Chalioris 2000). Other models combining two different models to predict the pre-cracking and the post-cracking stages of RC beams under torsion have been also proposed (Bernardo and Lopes 2008, 2011). The authors justify this methodology because experimentally it is clearly observed that the torsional behavior of a RC beam is very different before and after cracking. This observation reveals that a different load resisting mechanism exist in each case. Despite of the good predictions with such models, the referred methodology to build a theoretical model cannot be considered theoretically satisfactory, because a model mainly based on a single theory would be preferable.

When compared with many of the previously referred alternative models, it can be easily stated that both mathematical approach and solution procedure for VATM are much simpler. Furthermore, many of the previously referred models are only able to compute accurately the ultimate torsional behavior of RC beams. Nowadays, it is recognized that good predictions for low loading stages are also very important if one want to check the deformation of the beam and the stress/strain levels in the materials for the serviceability limit states. Design rules from codes of practice usually include such requirements.

Nowadays, prestress is widely used in many structural members, including in RC beams under high torsional loading. Prestress induces a compressive stress state in the concrete, which is combined with the shear stress induced by torsion. This biaxial stress state allow for a larger area of the concrete cross section to be effective. As a consequence, prestress increases the cracking torque, the torsional stiffness and also the torsional strength of the beams.

From the above reasons, new reliable and consistent analytical models are still need to predict accurately de global behavior of structural concrete beams under torsion, including for PC beams and for low loading stages. For this, some models based on the STA were refined and proposed to include the tensile concrete strength. Jeng and Hsu (2009) and Bernardo et al. (2012b, 2015a) extended, respectively, the Softened Membrane Model (SMM) (Hsu and Zhu 2002) and the VATM to RC beams under torsion. These analytical models, called Softened Membrane Model for Torsion (SMMT) (Jeng and Hsu 2009), Modified Variable Angle Truss-Model (MVATM) (Bernardo et al. 2012b) and Generalized Softened Variable Angle Truss-Model (GSVATM) (Bernardo et al. 2015a), are able to predict the entire torque (M_T)–twist (θ) curve of RC beams under torsion for all the loading stages. Among the previously referred models, the SMMT and the GSVATM are considered theoretically more consistent because they are based is one unique theory. The theoretical predictions from both models where shown to be in good agreement with the test data of RC plain beams under torsion, namely in terms of torsional stiffness, transition from the non-cracked stage to the cracked stage and also in terms of the maximum (resistance) torque.

Jeng et al. (2010) and Rodrigues (2011) extended successfully the SMMT for PC plain beams under torsion. More recently, both SMMT (Bernardo et al. 2013; Jeng 2015) and GSVATM (Vaz 2014) were also refined to provide good results for RC hollow beams under torsion. Good agreement with experimental data where also observed.

As previously referred, VATM is recognized as an analytical model which provides a simple physical understanding of the torsion phenomenon for structural concrete beams under torsion. The mathematical approach and the solution procedure is easy to understand and also to implement. GSVATM constitutes an extension of the VATM by including the additional contribution of the tensile concrete (concrete ties) in the perpendicular direction to the concrete struts. For this reason, when compared with SMMT which constitutes an extension of the SMM (Hsu and Zhu 2002), the mathematical treatment and the solution procedure is less complex.

Based on the foregoing, in this study, the GSVATM is extended to cover PC concrete beams under torsion. Uniform longitudinal prestressed is assumed since this constitutes the logical solution for beams under pure torsion, as also assumed in previous studies (Hsu and Mo 1985b; Jeng et al. 2010). The changes in the original GSVATM formulation and solution procedure are presented. The predictions obtained from the extended GSVATM are compared with experimental results of reference PC beams under torsion, which results are available in the literature. The comparative analysis is focused on the $M_T-\theta$ curves, namely for the cracking and ultimate key points.

Finally, it should be pointed that this study deals with a nonlinear analytical model (GSVATM) extended from the VATM and STA, which aims to predict the global behavior of PC beams under torsion. The interaction between torsion and prestressing effects is considered from the beginning of the calculation procedures, until

Table 1 Equilibrium and compatibility equations from GSVATM for RC beams (Bernardo et al. 2015a).

Plain truss analogy for a RC thin beam under shear:

$R = \sqrt{C^2 + T^2}$ (1)

$\beta = \arctan(T/C)$ (2)

$\gamma = \alpha + \beta$ (3)

$C = \sigma_2^c t_c d_v \cos\alpha$ (4)

$T = \sigma_1^c t_c d_v \sin\alpha$ (5)

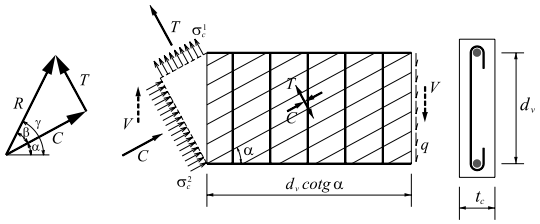

Space truss analogy for a RC box beam under torsion:

Equilibrium equations:

$M_T = \frac{2A_o R \sin\gamma}{d_v}$ (6)

$t_c = \frac{A_{sl} f_{sl}}{\sigma_2^c p_o} \frac{\cos\beta}{\cos\alpha \cos\gamma}$ for $\gamma = \alpha + \beta \leq 90°$ (7)

$\alpha = \arctan\left(\frac{\sqrt{F^2(\tan\beta)^2 + F(\tan\beta)^4 + F + (\tan\beta)^2}}{F(\tan\beta)^2 + 1}\right)$ with $F = \frac{A_{st} f_{st} p_o}{A_{sl} f_{sl} s}$ (8)

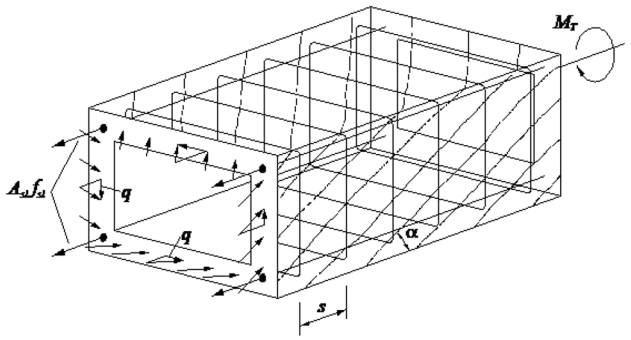

Compatibility equations:

$\varepsilon_{st} = \left(\frac{A_o^2 \sigma_2^c \sin\gamma}{p_o M_T \cos\beta \tan\alpha \sin\alpha} - \frac{1}{2}\right)\varepsilon_{2s}^c$ (9)

$\varepsilon_{sl} = \left(\frac{A_o^2 \sigma_2^c \sin\gamma}{p_o M_T \cos\beta \cot\alpha \sin\alpha} - \frac{1}{2}\right)\varepsilon_{2s}^c$ (10)

$\theta = \frac{\varepsilon_{2s}^c}{2t_c \sin\alpha \cos\alpha}$ (11)

$\varepsilon_{1s}^c = 2\varepsilon_1^c = 2\varepsilon_{sl} + 2\varepsilon_{st} + \varepsilon_{2s}^c$ (12)

the ultimate state. Particular models from codes of practice based on the STA were not described in the previous literature review. In fact, such models incorporates some simplifications to the original base model in order to practitioners be able to compute directly the most important key properties of RC and PC beams under torsion for design, such as the cracking and resistance torques. In such models incorporated in codes of practice, the prestressing treatment is different. For instance, in many national bridge design codes, the influence of prestressing is generally considered by adding an additional term to the torsional strength of PC beams, accounting for the "prestressing influence". More information about these simplified methods, for instance the concepts of "pressure-strain reduction" or the "prestressing influence term" to be add can be found in the literature, for instance (Nilson 1987; Hsu 1993).

2 The GSVATM for RC Beams

To allow for the reader to understand better the changes presented in Sect. 3, Table 1 presents the models and summarizes the main equations from the GSVATM for RC beams under torsion. The details about the derivation of the presented equations in Table 1 can be found in (Bernardo et al. 2015a). From a plain truss model for a RC thin beam element under shear V (which induces a shear flow q in the cross section) and from the VATM for a RC box beam element (see Table 1), the GSVATM incorporates the additional contribution of a concrete tie, with a tensile force T, perpendicular to the concrete strut with a compressive force C and with an angle α to the longitudinal axis. This angle is assumed to be equal to the angle of cracks (see Table 1). In the RC thin beam element under shear, the resultant force R, with an angle β (Eq. 2) with respect to C and an angle γ (Eq. 3) to the longitudinal axis, is computed from Eq. (1). The forces C (Eq. 4) and T (Eq. 5) are the resultants of the compressive and tensile stress fields in concrete (σ_2^c and σ_1^c, respectively), with d_v being the distance between centres of the longitudinal bars and t_c the width of the cross section (see Table 1), which is assumed to be equal to the width of the compressive and tensile concrete stress field (concrete strut and concrete tie, respectively).

The outer shell of a RC beam element under torsion (box beam) can be modelled as the union of four thin beam elements under shear equals to the referred above (see Table 1). Bredt's thin tube theory is used to relate the torsional moment M_T with the circulatory shear flow q. From this box beam element, a set of three equilibrium equations (see Table 1) are derived to compute the torsional moment, M_T (Eq. 6), the effective thickness t_c of the concrete strut and tie (Eq. 7) and the angle α of the inclined concrete struts to the longitudinal axis of the beam (Eq. 8). Equation (7) must be multiplied by (-1) if $\gamma = \alpha + \beta > 90°$. In these equations, A_o is the area enclosed by the center line of the shear flow (which is assumed to coincides with the center line of the walls: $A_o = (x - t_c)(y - t_c)$, with x and y being the minor and major outer dimension of the rectangular section), p_o is the perimeter of the center line of the shear flow ($p_o = 2(x - t_c) + 2(y - t_c)$), A_{sl} is the total area of longitudinal steel, A_{st} is the area of one bar of the transverse steel, s is the longitudinal spacing of the transverse reinforcement, f_{sl} and f_{st} are the stresses in the longitudinal and transverse reinforcement, respectively.

A set of three compatibility equations (see Table 1) are also derived to compute the strain in the transverse reinforcement, ε_{st} (Eq. 9), and longitudinal reinforcement, ε_{sl} (Eq. 10), as well as the twist per unit length θ (Eq. 11). An additional invariant equation which relates the strains is also derived (Eq. 12). In these equations, ε_{2s}^c is the maximum compressive strain at the surface of the strut, ε_1^c and ε_2^c are the average strains in the concrete tie and strut, respectively. The strains in the concrete tie and strut are computed considering the strain gradient due to the bending of walls (see Table 2).

To model the behavior of the compressive concrete in the diagonal struts, a smeared $\sigma - \varepsilon$ relationship must be adopted to consider the influence of the softening effect. In addition, to model the behavior of the tensile concrete in the diagonal ties and non-prestress steel bars in tension, smeared $\sigma - \varepsilon$ relationships must also be adopted to consider the influence of the stiffening effect.

From previous studies, Bernardo et al. (2012a) and Bernardo and Andrade (2017), by using the VATM to predict the ultimate behavior of RC and PC beams under torsion, found that, for concrete in compression, the $\sigma - \varepsilon$ relationship proposed by Belarbi and Hsu (1994) (Eqs. 13, 14 in Table 2) with softening factors ($\beta_* = \beta_\sigma = \beta_\varepsilon$, both for the peak stress and corresponding strain) proposed by Zhang and Hsu (1998) (Eqs. 15–18) provided good results for the ultimate stage, namely for the resistance torque and the corresponding twist. In addition, Nobre (2014) found that, for concrete in tension, the $\sigma - \varepsilon$ relationship proposed by Belarbi and Hsu (1994), modified by Jeng and Hsu (2009) and by Bernardo et al. (2013) for RC plain and hollow beams under torsion, respectively (Eqs. 19–23), provided good results for the cracking torque and corresponding twist. In Table 2, f_c' is the uniaxial concrete compressive strength, ε_o is the strain corresponding to f_c', ρ_l is the longitudinal reinforcement ratio ($\rho_l = A_{sl}/A_c$, with $A_c = xy$), ρ_t is the transverse reinforcement ratio ($\rho_l = A_{st}u/A_c s$, with $u = 2x + 2y$), f_{ly} and f_{ty} are the yielding stress for the longitudinal and transverse reinforcement, respectively, E_c is the Young's Modulus for concrete, f_{cr} is the concrete cracking stress and ε_{cr} is the strain corresponding to f_{cr}.

The stress in the diagonal concrete strut σ_2^c is defined as the average stress of a non-uniform stress diagram (Eq. 24, Table 2) due to the gradient of the strains, which in turn occurs due to the bending of the walls (Table 2). Similarly, the stress in the diagonal concrete tie σ_1^c is also defined as the average stress of a non-uniform stress diagram (Eq. 27, Table 2). In Eqs. (24) and (27), parameters k_2^c (Eqs. 25, 26) and k_1^c (Eqs. 28, 29) represent the average compressive and tensile stresses, respectively, and can be obtained by integrating Eqs. (13), (14) and (19), (20), respectively.

To model the behavior of the steel bars in tension, a smeared $\sigma - \varepsilon$ relationship must be adopted to consider the stiffening effect. In Bernardo et al. (2012a), Bernardo and Andrade (2017) it was also found that, for non-prestress steel bars, the $\sigma - \varepsilon$ relationship proposed by Belarbi and Hsu (1994) (Eqs. 30–32 in Table 2) provided good results. In Table 2, f_s and ε_s are the stress and strain in the steel bars, respectively, E_s is the Young's Modulus for steel, f_y is the yielding stress of steel bars and ρ is the reinforcement ratio.

The $\sigma - \varepsilon$ relationships referred above and presented in Table 2 (concrete in compression and tension, non-prestress steel bars in tension) were incorporated in the GSVATM (Bernardo et al. 2015a; Vaz 2014), which proved to give good results when compared to experimental data.

The solution procedure for the GSVATM, to compute the theoretical $M_T - \theta$ curve, is based on a trial-and-error technique, since some unknowns and interdependent variables exist at the starting of the calculations. The input value to starts the calculation procedure is the strain at the outer fiber of the concrete strut, $\varepsilon_{2s}^c = 2\varepsilon_2^c$ (see Table 2). The details of the solution algorithm for the GSVATM can be found in (Bernardo et al. 2015a).

The equations of the GSVATM and the solution algorithm are modified in this study for PC beams.

Table 2 $\sigma-\varepsilon$ relationships for concrete and steel.

Concrete in compression (Belarbi and Hsu 1994; Zhang and Hsu 1998):

$$\sigma_2^c = \beta_\sigma f_c' \left[2\left(\frac{\varepsilon_2^c}{\beta_\varepsilon \varepsilon_o}\right) - \left(\frac{\varepsilon_2^c}{\beta_\varepsilon \varepsilon_o}\right)^2\right] \text{ if } \varepsilon_2^c \le \beta_\varepsilon \varepsilon_o \quad (13)$$

$$\sigma_2^c = \beta_\sigma f_c' \left[1 - \left(\frac{\varepsilon_2^c - \beta_\varepsilon \varepsilon_o}{2\varepsilon_o - \beta_\varepsilon \varepsilon_o}\right)^2\right] \text{ if } \varepsilon_2^c > \beta_\varepsilon \varepsilon_o \quad (14)$$

$$\beta_* = \beta_\sigma = \beta_\varepsilon = \frac{R(f_c')}{\sqrt{1+\frac{400\varepsilon_1^c}{\eta'}}} \quad (15)$$

$$\eta = \frac{\rho_l f_{ly}}{\rho_t f_{ty}} \quad (16)$$

$$\begin{cases} \eta \le 1 \Rightarrow \eta' = \eta \\ \eta > 1 \Rightarrow \eta' = 1/\eta \end{cases} \quad (17)$$

$$R(f_c') = \frac{5.8}{\sqrt{f_c' \text{ (MPa)}}} \le 0.9 \quad (18)$$

Concrete in tension (Jeng and Hsu 2009; Bernardo et al. 2013; Belarbi and Hsu 1994):

$$\sigma_1^c = E_c \varepsilon_1^c \text{ if } \varepsilon_1^c \le \varepsilon_{cr} \quad (19)$$

$$\sigma_1^c = f_{cr}\left(\frac{\varepsilon_{cr}}{\varepsilon_2^c}\right)^{0.4} \text{ if } \varepsilon_1^c > \varepsilon_{cr} \quad (20)$$

$$k_2^c = \frac{\varepsilon_{2s}^c}{\beta_\varepsilon \varepsilon_o} - \frac{(\varepsilon_{2s}^c)^2}{3(\beta_\varepsilon \varepsilon_o)^2} \quad (21)$$

$$E_c = 3875\, K \sqrt{f_c' (\text{MPa})} \quad (22)$$

$$\varepsilon_{cr} = 0.00008\, K \quad K = 1.45 \text{ or } 1.24 \text{ (plain or hollow)} \quad (23)$$

Equations for stress in the concrete diagonal struts (Bernardo et al. 2015a):

$$\sigma_2^c = k_2^c \beta_\sigma f_c' \quad (24)$$

$$k_2^c = \frac{\varepsilon_{2s}^c}{\beta_\varepsilon \varepsilon_o} - \frac{(\varepsilon_{2s}^c)^2}{3(\beta_\varepsilon \varepsilon_o)^2} \text{ if } \varepsilon_{2s}^c \le \beta_\varepsilon \varepsilon_o \quad (25)$$

$$k_2^c = 1 - \frac{\beta_\varepsilon \varepsilon_o}{3\varepsilon_{2s}^c} - \frac{(\varepsilon_{2s}^c - \beta_\varepsilon \varepsilon_o)^3}{3\varepsilon_{2s}^c (2\varepsilon_o - \beta_\varepsilon \varepsilon_o)^2} \text{ if } \varepsilon_{2s}^c > \beta_\varepsilon \varepsilon_o \quad (26)$$

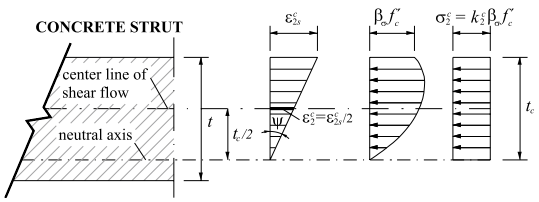

Equations for stress in the concrete diagonal ties (Bernardo et al. 2015a):

$$\sigma_1^c = k_1^c f_{cr} \quad (27)$$

$$k_1^c = \frac{\varepsilon_{1s}^c}{2\varepsilon_{cr}} \text{ if } \varepsilon_{1s}^c \le \varepsilon_{cr} \quad (28)$$

$$k_1^c = \frac{\varepsilon_{cr}}{2\varepsilon_{1s}^c} + \frac{(\varepsilon_{cr})^{0.4}}{0.6\varepsilon_{1s}^c}\left[(\varepsilon_{1s}^c)^{0.6} - (\varepsilon_{cr})^{0.6}\right] \text{ if } \varepsilon_{1s}^c > \varepsilon_{cr} \quad (29)$$

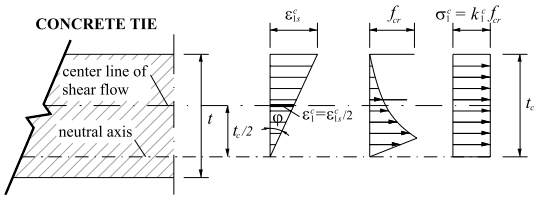

Non-prestress steel bars in tension (Belarbi and Hsu 1994):

$$f_s = \frac{0.975 E_s \varepsilon_s}{\left[1+\left(\frac{1.1 E_s \varepsilon_s}{f_y}\right)^m\right]^{\frac{1}{m}}} + 0.025 E_s \varepsilon_s \quad (30)$$

$$m = \frac{1}{9B-0.2} \le 25 \quad (31)$$

$$B = \frac{1}{\rho}\left(\frac{f_{cr}}{f_y}\right)^{1.5} \quad (32)$$

Prestress steel bars in tension (Hsu and Mo 1985b):

$$f_p = E_p \varepsilon_p \text{ if } \varepsilon_p \le \varepsilon_{p0.1\%} = f_{p0.1\%}/E_p \quad (33)$$

$$f_p = \frac{E_p \varepsilon_p}{\left[1+\left(\frac{E_p \varepsilon_p}{f_{pt}}\right)^{4.38}\right]^{\frac{1}{4.38}}} \text{ if } \varepsilon_p > \varepsilon_{p0.1\%} \quad (34)$$

3 The GSVATM for PC Beams

3.1 Assumptions to Incorporate Prestress

Longitudinal prestress is favourable for the torsional behavior of RC beams under torsion (Jeng et al. 2010; Bernardo et al. 2013). The combined action of longitudinal prestress and torsion induces a biaxial stress state (initial longitudinal compressive stress + shear stress) which increases the cracking torque of the beam. In addition,

after concrete decompression the PC beam behaves like a current RC beam and longitudinal prestress reinforcement behaves as ordinary reinforcement, contributing to increase the resistance torque. Concrete decompression occurs when the strain in the non-prestress longitudinal reinforcement, initially in compression due to prestress, becomes zero due to the increasing torque.

To include the effect of longitudinal prestress, the following assumptions are made to extend the GSVATM for PC beams under torsion:

- The calculation of the $M_T-\theta$ curve for the pre-decompression stage is not relevant because the small associated part of the $M_T-\theta$ curve is perfectly linear. Then, it is assumed that GSVATM will only start the calculation procedure after the concrete decompression. This procedure is similar to the same one assumed by Hsu and Mo (1985b) to extend the VATM to PC beams under torsion. This assumption allows to simplificate the solution procedure because the strain and stress gradients in the concrete strut and tie do not need to include the initial compressive stress state in concrete due to prestress. The modelling of this initial stress state would complicate needlessly the calculation procedure for the very low loading stages (Jeng et al. 2010);
- Related with the previous assumption, it should be referred that the influence of long term response of the PC beams was neglected in this study, as also assumed by Jeng et al. (2010). In such study, the pre-decompression response of the PC beams was computed and the stress variation in the concrete was only due to the incremental torsional loading. However, it should be referred that stress variations in the concrete decompression stage in fact exists due to viscous effects in the concrete, in accordance with the long term response of structural concrete structures (Price and Anderson 1992; Johnson 1994; Ascione et al. 2011; Berardi and Mancusi 2012, 2013);
- From the referred previously, despite the initial compressive stress state due to prestress is not directly modelled to compute the strain and stress states in concrete before decompression, it must be considered to compute the initial strain in the longitudinal prestress and non-prestress reinforcement, in order to compute the strain at concrete decompression. In addition, the torsional moment corresponding to the tensile strength of concrete, that is the cracking torque, must be corrected to include the favourable effect due to prestress. This correction is performed by using a simple prestress factor;
- After the concrete decompression, and as for the non-prestress reinforcement, longitudinal prestress reinforcement participates for the longitudinal equilibrium of the beam. Then, equilibrium equations must incorporate the force in the prestress reinforcement;
- An additional $\sigma-\varepsilon$ relationship for the prestress steel reinforcement in tension must be implemented to model the behavior of this material and compute the stresses.

3.2 Changes in the GSVATM

To consider indirectly the influence in the non-cracked stage (for $\varepsilon_1^c \leq \varepsilon_{cr}$) of the initial compressive stress state in the concrete due to prestress, Eq. (6) (Table 1) to compute the torsional moment, M_T, is multiplied by a prestress factor γ_p:

$$M_T = \gamma_p \frac{2A_o R \sin\gamma}{d_v} \tag{35}$$

$$\gamma_p = \begin{cases} \sqrt{1+10\dfrac{f_{cp,i}}{f_c'}} & \text{if } \varepsilon_1^c \leq \varepsilon_{cr} \\ 1 & \text{if } \varepsilon_1^c > \varepsilon_{cr} \end{cases} \tag{36}$$

In Eq. (36), $f_{cp,i}$ is the initial compressive stress in concrete due to the longitudinal prestress. This prestress factor was proposed by Hsu (1984), based on Cowan's failure criterion. This prestress factor proved to be a simple parameter to correct the cracking torque due to prestress and has been used in previous analytical models for PC beams under torsion (Hsu 1984; Lopes and Bernardo 2014; Andrade and Bernardo 2013). From Eqs. (35) and (36), the maximum torsional moment for which the prestress factor is higher than unity corresponds to the cracking torque M_{Tcr} (which occurs when $\varepsilon_1^c = \varepsilon_{cr}$). This simplified procedure to correct the torsional moment is acceptable because in the non-cracked stage the $M_T-\theta$ curve is linear. In this stage, the most important key point of the $M_T-\theta$ curve is the upper limit, with coordinates (θ_{cr};M_{Tcr}).

For consistency, in the non-cracked stage, the twists θ must also be multiplied by γ_p, in order to maintain unchanged the torsional stiffness in this stage. Then, Eq. (11) (Table 1) must also be corrected:

$$\theta = \gamma_p \frac{\varepsilon_{2s}^c}{2t_c \sin\alpha \cos\alpha} \tag{37}$$

To account for the initial deformation due to prestress, after the concrete decompression, the strain in the longitudinal prestress reinforcement, ε_p, can be calculated as follows:

$$\varepsilon_p = \varepsilon_{dec} + \varepsilon_{sl} \tag{38}$$

where ε_{dec} = decompression strain; ε_{sl} = strain in the longitudinal non-prestress reinforcement due to the external torque.

The decompression strain ε_{dec} is the sum of the initial tensile strain in the prestress reinforcement due to prestress, $\varepsilon_{p,i}$, with the strain in the longitudinal non-prestress reinforcement necessary to reach the decompression (Eq. 39). This last one is equal, in modulus, to the initial compressive strain in the longitudinal non-prestress reinforcement due to prestress, $\varepsilon_{sl,i}$. It should be referred that when concrete decompression occurs, $\varepsilon_{sl} = 0$

$$\varepsilon_{dec} = \varepsilon_{p,i} + \varepsilon_{sl,i} \tag{39}$$

By using Hooke's law and based on the homogenized cross section, the initial strains are computed as follows:

$$\varepsilon_{p,i} = \frac{f_{p,i}}{E_p} \tag{40}$$

$$\varepsilon_{sl,i} = \frac{A_p f_{p,i}}{A_{sl}(E_s - E_c) + \left(A_c - A_h - A_p\right)E_c} \tag{41}$$

where $f_{p,i}$ = initial stress in the prestress reinforcement, due to prestress; E_p = Young's Modulus for prestress steel; A_p = total area of longitudinal prestress reinforcement; A_h = area of the hollow part for hollow sections (for plain sections, $A_h = 0$).

Since the calculation procedure of the GSVATM starts at concrete decompression ($\varepsilon_{sl} = 0$), Eqs. (9, 10) (Table 1) remain valid to compute the strains in the longitudinal and transverse non-prestress reinforcement.

To start the calculation procedure (Sect. 3.3), the input value is the strain at the outer fiber of the concrete strut, $\varepsilon_{2s}^c = 2\varepsilon_2^c$ (see Table 2). Since the calculation procedure starts at concrete decompression, ε_{2s}^c must starts from zero.

After the concrete decompression, PC beams behaves as RC beams. Then, the participation of the longitudinal prestress reinforcement must be considered for the longitudinal equilibrium. For this, Eq. (7) (Table 1), to compute the effective width of the concrete strut and tie, must include the force in the longitudinal prestress reinforcement, $A_p f_p$:

$$t_c = \frac{A_{sl} f_{sl} + A_p f_p}{\sigma_2^c p_o} \frac{\cos\beta}{\cos\alpha \cos\gamma} \text{ for } \gamma = \alpha + \beta \leq 90^\circ \tag{42}$$

Parameter F in Eq. (8) (Table 1), to compute the angle of the concrete strut to the longitudinal axis, must also include the force in the longitudinal prestress reinforcement, $A_p f_p$:

$$\alpha = \arctan\left(\frac{\sqrt{F^2(\tan\beta)^2 + F(\tan\beta)^4 + F + (\tan\beta)^2}}{F(\tan\beta)^2 + 1}\right) \quad \text{with } F = \frac{A_{st} f_{st} p_o}{\left(A_{sl} f_{sl} + A_p f_p\right)s} \tag{43}$$

To characterize the behavior of the materials, the same $\sigma - \varepsilon$ relationships assumed in the GSVATM for RC beams (Bernardo et al. 2015a) are also used here. However, for concrete in compression, parameter η (Eq. (16), Table 2), which accounts for the ratio between the longitudinal and transverse resistance forces in the reinforcements, must be rewritten to account for the additional resistance force of the longitudinal prestress reinforcement:

$$\eta = \frac{\rho_l f_{sly} + \rho_p f_{p0.1\%}}{\rho_t f_{sty}} \tag{44}$$

where ρ_p = longitudinal prestress reinforcement ratio ($\rho_p = A_p/A_c$); $f_{p0.1\%}$ = proportional conventional limit stress to 0.1% for the longitudinal prestressing steel.

To model the behavior of the prestress steel reinforcement in tension, a $\sigma - \varepsilon$ relationship must be adopted. Bernardo and Andrade (2017) found that the $\sigma - \varepsilon$ relationship for prestress reinforcement in tension proposed by Ramberg–Osgood (Eqs. 33, 34, Table 2), which was also used by Hsu and Mo (1985b) for the VATM, provides good results. This $\sigma - \varepsilon$ relationship is also adopted for this study. In Table 2, f_p and ε_p are the stress and strain in the prestress steel reinforcement, respectively, E_p is the Young's Modulus for prestressing steel, $\varepsilon_{p0.1\%}$ is the strain corresponding to $f_{p0.1\%}$ and f_{pt} is the tensile strength of prestress steel reinforcement.

3.3 Solution Procedure

As for the GSVATM for RC beams (Bernardo et al. 2015a), the solution procedure for the GSVATM for PC beams to compute the theoretical $M_T - \theta$ curve is based on a trial-and-error technique. This is because some unknown and interdependent variables must be assumed or estimated at the starting of the calculations. Figure 1 shows the flowchart for the iterative calculation algorithm used in this study. The first input value to starts

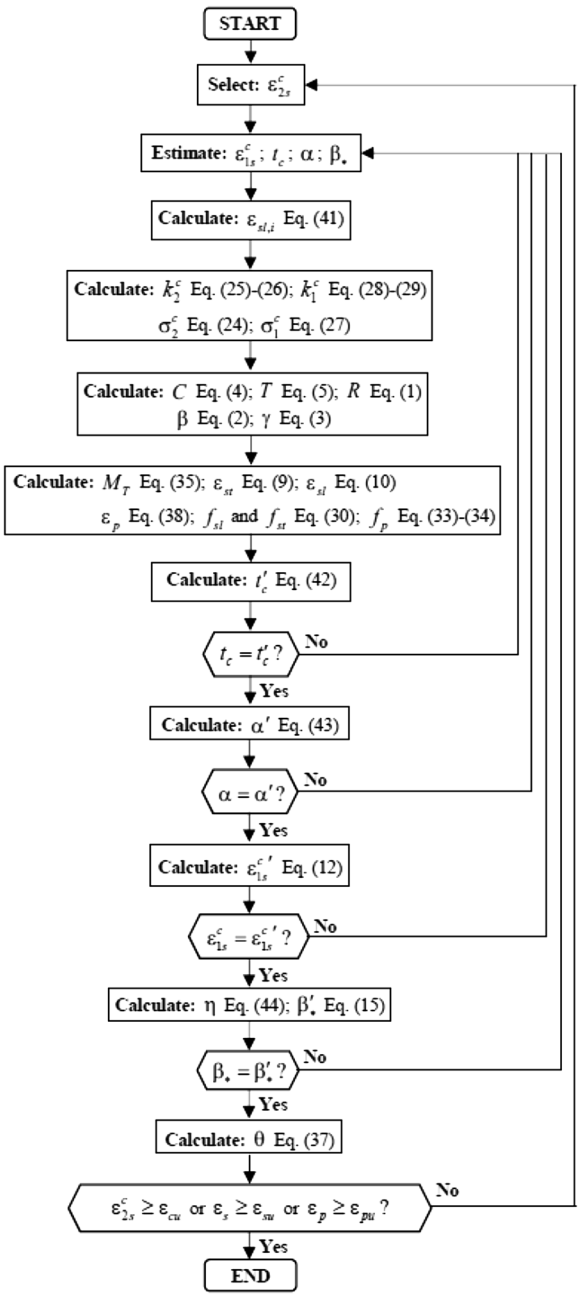

Fig. 1 Flowchart to compute the $M_T-\theta$ curve with GSVATM for PC beams.

the calculation procedure, which is incremented for each new cycle, is the strain at the outer fiber of the concrete struts ε_{2s}^{c}. Each cycle of the solution procedure corresponds to a solution point of the $M_T-\theta$ curve, with coordinates (θ; M_T).

The end point of the theoretical $M_T-\theta$ curve corresponds to the theoretical failure of the PC beam under torsion. This one occurs when the maximum compressive strain at the outer fiber of the concrete strut, ε_{2s}^{c}, reaches its conventional ultimate value. ε_{cu}, or when the tensile strain for the reinforcements, ε_s or ε_p, reaches its conventional ultimate value, ε_{su} or ε_{pu}. In this study, these conventional values are defined from Eurocode 2 procedures (NP EN 1992-1-1 1992).

In this study, the solution procedure was implemented with computing language Delphi. The resulting computer program was used to compute the $M_T-\theta$ curve of several reference PC beams under torsion, as presented in Sect. 4.

4 Comparative Analysis with Experimental Results and Codes of Practice

In this section, the theoretical results obtained from the GSVATM for PC beams are compared with the experimental results from reference PC beams found in the literature and also with the predictions from some codes of practice which uses simplified methods to account for the influence of prestressing, as referred in the end of Sect. 1. The objective is to check the degree of accuracy of the GSVATM, when compared with experimental results and also with the predictions of simplified models for design, such as the ones incorporated in the codes of practice. The comparative analysis is performed by comparing some key points of the experimental and theoretical $M_T-\theta$ curves, namely the cracking torque (θ_{cr}; M_{Tcr}) and ultimate (maximum) torque (θ_u; T_u), as also performed in previous studies (Jeng and Hsu 2009; Bernardo et al. 2015a). These key points allow to check if the extended GSVATM provides good predictions for the low and high loading stages.

The following reference codes of practice are considered: American code ACI 318R-14 (ACI Committee 318 2014), European Codes MC 10 (CEB-FIP MODEL 2010) and EC 2 (NP EN 1992-1-1 1992), and Canadian Standard CAN3-A23.3-14 (CSA Standard 2014).

For the comparative analysis with experimental data, twenty-nine PC beams (with longitudinal and uniform prestress) with rectangular cross section and tested under torsion were collected from previous studies, namely: Mitchell and Collins (1974), El-Degwy and McMullen (1985), Hsu and Mo (1985b), Wafa et al. (1995) and Bernardo et al. (2013). However, not all the collected beams can be considered trustworthy for the comparative analysis focused on their global behavior (not only for the resistance torque). In general, in experimental studies the authors present the average twist for all the beam length and not the twist at the critical zone of the beam. In slender beams, the theoretical twists, usually computed from a section analysis, can be very different when compared with the experimental twists. When compared with the

Table 3 Properties of reference PC beams.

Beam	Section[a]	x (cm)	y (cm)	t (cm)	A_{sl} (cm^2)	A_{st}/s (cm^2/m)	A_p (cm^2)	ρ_l (%)	ρ_t (%)	ρ_p (%)	f_c (MPa)	f_{sly} (MPa)	f_{sty} (MPa)	$f_{p0.1\%}$ (MPa)	$f_{p,i}$ (MPa)	f_{cp} (MPa)
P2 (Mitchell and Collins 1974)	H	35.6	43.2	8.9	5.6	7.4	4.6	0.37	0.61	0.29	32.9	407	407	1476	1145	4.9
P3 (Mitchell and Collins 1974)	H	35.6	43.2	–	4.3	7.4	1.2	0.28	0.63	0.07	34.0	328	328	1476	1145	0.9
P8 (Hsu and Mo 1985b)	H	25.4	38.1	–	5.2	22.6	9.6	0.53	2.90	1.02	31.0	334	336	959	690	6.8
D1 (Bernardo et al. 2013)	H	60.0	60.0	11.4	23.8	11.2	4.2	0.66	0.68	0.11	80.8	724	715	1670	640	1.8
D2 (Bernardo et al. 2013)	H	60.0	60.0	11.5	23.8	11.2	5.6	0.66	0.69	0.15	58.8	724	715	1670	1100	3.1
PA1R (El-Degwy and McMullen 1985)	P	25.4	25.4	–	2.8	4.5	0.9	0.40	0.80	0.20	43.6	435	310	1638	1207	1.7
PA2 (El-Degwy and McMullen 1985)	P	25.4	25.4	–	5.2	7.7	1.5	0.80	1.40	0.20	45.6	483	310	1663	1207	2.8
PA3 (El-Degwy and McMullen 1985)	P	25.4	25.4	–	8.0	7.9	2.1	1.20	1.40	0.40	41.8	389	435	1744	1303	4.2
PA4 (El-Degwy and McMullen 1985)	P	25.4	25.4	–	11.4	11.0	3.0	1.80	2.00	0.40	42.2	419	435	1709	1303	6.0
PB1 (El-Degwy and McMullen 1985)	P	17.8	35.6	–	2.8	4.5	0.9	0.40	0.80	0.20	45.8	435	310	1638	1207	1.8
PB2 (El-Degwy and McMullen 1985)	P	17.8	35.6	–	5.2	7.7	1.5	0.80	1.50	0.30	45.8	483	310	1663	1207	2.9
PB3 (El-Degwy and McMullen 1985)	P	17.8	35.6	–	8.0	7.5	2.1	1.30	1.40	0.30	45.5	389	435	1744	1303	4.2
PB4 (El-Degwy and McMullen 1985)	P	17.8	35.6	–	11.4	10.2	3.0	1.80	2.00	0.50	45.5	419	435	1709	1303	6.1
PC1 (El-Degwy and McMullen 1985)	P	14.6	43.8	–	2.8	3.9	0.9	0.40	0.80	0.20	42.2	435	310	1638	1207	1.8
PC2 (El-Degwy and McMullen 1985)	P	14.6	43.8	–	5.2	6.9	1.5	0.80	1.50	0.20	45.1	483	310	1663	1207	2.8
PC3 (El-Degwy and McMullen 1985)	P	14.6	43.8	–	8.0	6.8	2.1	1.30	1.40	0.30	41.3	389	435	1744	1303	4.2
PC4 (El-Degwy and McMullen 1985)	P	14.6	43.8	–	11.4	9.5	3.0	1.80	2.00	0.40	42.1	419	435	1709	1303	6.1
H3AR (Wafa et al. 1995)	P	14.0	42.0	–	8.0	10.3	4.0	1.40	2.00	0.60	92.2	487	390	1816	1366	8.3
H2A (Wafa et al. 1995)	P	17.0	34.0	–	8.0	12.6	4.0	1.40	2.20	0.70	91.9	487	390	1816	1338	8.7
H1AR (Wafa et al. 1995)	P	24.0	24.0	–	8.0	12.6	4.0	1.40	2.10	0.70	94.7	487	390	1816	1374	6.4
H3B (Wafa et al. 1995)	P	14.0	42.0	–	6.2	5.6	2.1	1.00	1.10	0.40	91.5	374	387	1841	1309	4.0
H2B (Wafa et al. 1995)	P	17.0	34.0	–	6.2	6.0	2.1	1.10	1.10	0.30	95.6	374	387	1841	1344	4.3
H1B (Wafa et al. 1995)	P	24.0	24.0	–	6.2	6.5	2.1	1.10	1.10	0.30	89.8	374	387	1841	1258	4.3
M3A (Wafa et al. 1995)	P	14.0	42.0	–	8.0	10.3	4.0	1.40	2.00	0.60	69.9	487	390	1816	1036	6.5
M2A (Wafa et al. 1995)	P	17.0	34.0	–	8.0	11.3	4.0	1.40	2.00	0.70	70.1	487	390	1816	1021	6.2
M1A (Wafa et al. 1995)	P	24.0	24.0	–	8.0	12.6	4.0	1.40	2.10	0.70	72.5	487	390	1816	1053	6.4
M3B (Wafa et al. 1995)	P	14.0	42.0	–	6.2	5.6	2.1	1.00	1.10	0.40	69.3	374	387	1841	991	3.2
M2B (Wafa et al. 1995)	P	17.0	34.0	–	6.2	6.0	2.1	1.10	1.10	0.30	69.7	374	387	1841	979	3.3
M1B (Wafa et al. 1995)	P	24.0	24.0	–	6.2	6.5	2.1	1.10	1.10	0.30	72.0	374	387	1841	1008	3.2

[a] *P* plain section, *H* hollow section.

theoretical results from the GSVATM, the PC beams from Wafa et al. (1995) show very different values for the twists for all the loading stages, despite good agreement is observed for the torsional moments. This probably explains why some authors did not consider these PC beams in their comparative analysis, for instance Jeng et al. (2010). For this reason, in this study the PC beams from Wafa et al. (1995) will not be used for comparative analysis with respect to the twists, but only with the torsional moments.

Table 3 presents the main properties of the 29 reference PC beams, which are need to compute the $M_T-\theta$ curves from the GSVATM, namely: the width (x) and height (y) of the cross section, the thickness of the walls (t) for hollow sections, the total area of longitudinal non-prestress reinforcement (A_{sl}), the distributed area of one unit of the transverse reinforcement (A_{st}/s, with A_{st} the area for one bar of the transverse reinforcement and s the longitudinal spacing between hoops), the total area of longitudinal prestress reinforcement (A_p), the longitudinal non-prestress reinforcement ratio ($\rho_l = A_{sl}/xy$), the transversal reinforcement ratio ($\rho_t = A_{st}u/A_c s$, with $u = x + y$ and $A_c = xy$), the longitudinal prestress reinforcement ratio ($\rho_p = A_p/xy$), the average concrete compressive strength (f_c), the average yielding stress for non-prestress longitudinal and transverse reinforcement (f_{sly} and f_{sty}), the proportional conventional limit stress to 0.1% of the prestress reinforcement ($f_{p0.1\%}$), the initial stress in the prestress reinforcement ($f_{p,i}$) and in the concrete (f_{cp}) due to prestress.

Some of the properties for the materials are usually not given by the authors, namely the average Young's Modulus for steel reinforcement and concrete (E_s, E_p and E_c). For concrete, the Young's Modulus was computed from Eurocode 2 (NP EN 1992-1-1 1992) based on the correlation with f_c. For non-prestress steel reinforcement the Young's Modulus was considered equal to 200 GPa (NP EN 1992-1-1 1992). For prestress steel reinforcement the Young's Modulus was considered to be in the range 190–200 GPa, depending on the solution used for this reinforcement (NP EN 1992-1-1 1992).

For the reference PC beams, Table 4 presents the experimental and theoretical values of the cracking torque ($M_{Tcr,\mathrm{exp}}$ and $M_{Tcr,\mathrm{th}}$), ultimate (maximum) torque ($M_{Tu,\mathrm{exp}}$ and $M_{Tu,\mathrm{th}}$) and corresponding twists ($\theta_{Tcr,\mathrm{exp}}$, $\theta_{Tcr,\mathrm{th}}$, $\theta_{Tu,\mathrm{exp}}$, $\theta_{Tu,\mathrm{th}}$). Table 5 also presents the ratios $M_{Tcr,\mathrm{exp}}/M_{Tcr,\mathrm{th}}$, $M_{Tu,\mathrm{exp}}/M_{Tu,\mathrm{th}}$, $\theta_{Tcr,\mathrm{exp}}/\theta_{Tcr,\mathrm{th}}$ and $\theta_{Tu,\mathrm{exp}}/\theta_{Tu,\mathrm{th}}$, as well as the corresponding average values ($\bar{x}$), sample standard deviations (s) and coefficients of variation (cv). As previously referred, the experimental results for the reference PC beams from Wafa et al. (1995) are only compared with respect to the torsional moments.

Table 4 shows that the theoretical cracking torques (M_{Tcr}) are very close to the experimental ones ($\bar{x} = 1.02$). The degree of dispersion of the results is quite acceptable ($cv = 10.3\%$). The cracking twists (θ_{Tcr}) are underestimated ($\bar{x} = 1.60$) and the dispersion of the results is higher ($cv = 30.6\%$). These last results can probably be attributed to the very low values of the twists at this stage, which can lead to a larger variability of the experimental results due to the limitation of the transducers accuracy.

The results in Table 4 also show that the theoretical model predict very well the ultimate torque (M_{Tu}) for the PC beams ($\bar{x} = 0.98$), with a low degree of dispersion of the results ($cv = 8.8\%$). For the twist corresponding to the ultimate torque (θ_{Tu}), Table 5 shows that, in general, the theoretical model seems to slightly underestimate this parameter ($\bar{x} = 1.10$). The results also show higher dispersion ($cv = 20.3\%$). Ultimate deformations are usually predicted with less accuracy by theoretical models due to the complex nonlinear behavior of RC members at the ultimate stage. This is also true for RC and PC beams under torsion, as observed in previous studies (Jeng and Hsu 2009; Bernardo et al. 2012b, 2015a; Jeng et al. 2010).

Since the cracking and ultimate twists are not very relevant for design purpose, the less positive results observed for these parameters can be considered not very important.

Figure 2 presents the experimental and theoretical $M_T-\theta$ curves for some reference PC beams analyzed in this study, as examples. Figure 2 shows that the global behavior of the PC beams under torsion is generally well captured by the GSVATM for PC beams, including the transition from the non-cracked stage to the cracked stage. It is also observed that the theoretical $M_T-\theta$ curves end prematurely when compared to the experimental ones. This is due to the assumed criteria to stop the calculation procedure (Sect. 3.3). As for the GSVATM for RC beams (Bernardo et al. 2015a), the $M_T-\theta$ curves in Fig. 2 show a descending branch immediately after the cracking torque, which is not experimentally observed. This behavior is related with the shape of the smeared $\sigma-\varepsilon$ relationship for the concrete in tension (see Table 2) after the peak stress (which corresponds to the cracking torque). A detailed discussion on this subject can be found in (Bernardo et al. 2015a). It should be referred that this behavior was also observed by Jeng et al. (2010) with the SMMT (GSVATM incorporates the same $\sigma-\varepsilon$ relationship for the tensile concrete).

For the same reference PC beams listed in Table 4, Table 5 presents the normative values of the cracking torque ($M_{Tcr,n}$) and ultimate (maximum) torque ($M_{Tu,n}$). For the cracking torque, only ACI 318R-14 (ACI Committee 318 2014) presents a specific equation for its calculation. For the corresponding twists to M_{Tcr} and M_{Tu},

Table 4 Comparative analysis for the cracking and ultimate key points—GSVATM.

Beam	$M_{Tcr,exp}$ (kN m)	$M_{Tcr,th}$ (kN m)	$\frac{M_{Tcr,exp}}{M_{Tcr,th}}$	$\theta_{Tcr,exp}$ (°/m)	$\theta_{Tcr,th}$ °/m	$\frac{\theta_{Tcr,exp}}{\theta_{Tcr,th}}$	$M_{Tu,exp}$ (kN m)	$M_{Tu,th}$ (kN m)	$\frac{M_{Tu,exp}}{M_{Tu,th}}$	$\theta_{Tu,exp}$ (°/m)	$\theta_{Tu,th}$ (°/m)	$\frac{\theta_{Tu,exp}}{\theta_{Tu,th}}$
P2 (Mitchell and Collins 1974)	58.0	55.4	1.05	0.14	0.09	1.55	87.1	84.5	1.03	2.80	1.86	1.50
P3 (Mitchell and Collins 1974)	41.2	44.4	0.93	0.21	0.10	2.06	55.8	71.4	0.78	3.14	2.60	1.21
P8 (Hsu and Mo 1985b)	45.2	47.6	0.95	0.24	0.21	1.13	61.8	67.4	0.92	1.89	1.66	1.14
D1 (Bernardo et al. 2013)	172.9	184.4	0.94	0.07	0.05	1.41	396.0	450.6	0.88	1.73	1.98	0.87
D2 (Bernardo et al. 2013)	184.7	178.7	1.03	0.07	0.08	0.89	447.7	434.2	1.03	1.93	1.68	1.15
PA1R (El-Degwy and McMullen 1985)	18.6	16.9	1.10	0.14	0.18	0.78	21.8	21.4	1.02	2.98	4.34	0.69
PA2 (El-Degwy and McMullen 1985)	22.8	23.1	0.99	0.61	0.23	2.71	29.3	31.5	0.93	2.87	2.85	1.01
PA3 (El-Degwy and McMullen 1985)	25.1	26.7	0.94	0.38	0.29	1.31	34.0	35.2	0.96	2.68	2.72	0.98
PA4 (El-Degwy and McMullen 1985)	26.3	28.6	0.92	0.29	0.26	1.09	37.4	40.0	0.94	2.95	2.37	1.24
PB1 (El-Degwy and McMullen 1985)	16.4	14.9	1.10	0.51	0.23	2.23	22.2	20.5	1.08	4.47	4.50	1.00
PB2 (El-Degwy and McMullen 1985)	18.9	17.0	1.11	0.43	0.23	1.87	27.5	29.7	0.93	2.75	3.24	0.85
PB3 (El-Degwy and McMullen 1985)	21.8	18.6	1.17	0.56	0.31	1.81	32.6	32.9	0.99	3.08	2.98	1.03
PB4 (El-Degwy and McMullen 1985)	24.1	22.3	1.08	0.44	0.26	1.68	37.6	36.9	1.02	2.63	2.55	1.03
PC1 (El-Degwy and McMullen 1985)	13.9	13.5	1.03	0.71	0.39	1.83	19.7	18.0	1.10	5.23	4.48	1.17
PC2 (El-Degwy and McMullen 1985)	17.2	19.3	0.89	0.33	0.22	1.54	28.6	26.5	1.08	3.38	3.46	0.98
PC3 (El-Degwy and McMullen 1985)	18.5	15.9	1.16	0.55	0.30	1.80	32.8	28.8	1.14	4.74	3.22	1.47
PC4 (El-Degwy and McMullen 1985)	21.6	22.7	0.95	0.50	0.32	1.55	38.7	33.5	1.16	3.84	2.71	1.42
H3AR (Wafa et al. 1995)	22.7	20.4	1.11	–	0.29	–	33.7	36.8	0.91	–	2.84	–
H2A (Wafa et al. 1995)	15.1	20.8	0.73	–	0.27	–	35.8	41.6	0.86	–	2.60	–
H1AR (Wafa et al. 1995)	31.6	27.7	1.14	–	0.25	–	38.4	44.0	0.87	–	2.34	–
H3B (Wafa et al. 1995)	20.7	22.6	0.91	–	0.37	–	26.4	26.8	0.98	–	3.31	–
H2B (Wafa et al. 1995)	27.1	29.2	0.93	–	0.37	–	29.5	29.1	1.01	–	2.90	–
H1B (Wafa et al. 1995)	29.9	27.8	1.07	–	0.37	–	31.3	30.7	1.02	–	2.85	–
M3A (Wafa et al. 1995)	19.6	17.9	1.09	–	0.36	–	30.0	32.6	0.92	–	2.87	–
M2A (Wafa et al. 1995)	27.0	28.8	0.94	–	0.44	–	31.9	35.3	0.91	–	2.58	–
M1A (Wafa et al. 1995)	31.5	33.1	0.95	–	0.33	–	35.4	39.1	0.91	–	2.37	–
M3B (Wafa et al. 1995)	18.3	15.5	1.18	–	0.38	–	24.7	24.6	1.01	–	3.48	–
M2B (Wafa et al. 1995)	26.2	24.5	1.07	–	0.41	–	26.2	26.3	1.00	–	3.11	–
M1B (Wafa et al. 1995)	26.8	27.5	0.97	–	0.43	–	28.9	28.6	1.01	–	2.88	–
		$\bar{x}=1.02$			$\bar{x}=1.60$			$\bar{x}=0.98$			$\bar{x}=1.10$	
		$s=0.10$			$s=0.49$			$s=0.09$			$s=0.22$	
		$cv=10.3\%$			$cv=30.6\%$			$cv=8.8\%$			$cv=20.3\%$	

Table 5 Comparative analysis for the cracking and ultimate torques—codes of practice.

Beam	ACI 318R-14 (ACI Committee 318 2014)				MC 10 (CEB-FIP MODEL 2010)		EC 2 (NP EN 1992-1-1 1992)		CAN3-A23.3-14 (CSA Standard 2014)	
	$M_{Tcr,n}$ (kN m)	$\frac{M_{Tcr,exp}}{M_{Tcr,n}}$	$M_{Tu,n}$ (kN m)	$\frac{M_{Tu,exp}}{M_{Tu,n}}$	$M_{Tu,n}$ (kN m)	$\frac{M_{Tu,exp}}{M_{Tu,n}}$	$M_{Tu,n}$ (kN m)	$\frac{M_{Tu,exp}}{M_{Tu,n}}$	$M_{Tu,n}$ (kN m)	$\frac{M_{Tu,exp}}{M_{Tu,n}}$
P2 (Jeng et al. 2010)	137.18	0.42	68.11	1.28	111.28	0.78	112.13	0.78	142.08	0.613
P3 (Jeng et al. 2010)	88.74	0.46	46.26	1.21	100.27	0.56	54.41	1.03	68.95	0.809
P8 (Hsu and Mo 1985b)	75.08	0.60	30.86	2.00	36.60	1.69	116.31	0.53	64.67	0.956
D1 (Bernardo et al. 2015c)	502.16	0.34	505.64	0.78	730.46	0.54	594.78	0.67	753.65	0.525
D2 (Bernardo et al. 2015c)	515.56	0.36	548.28	0.82	612.36	0.73	644.94	0.69	817.21	0.548
PA1R (Bernardo et al. 2013)	30.55	0.61	18.23	1.20	20.28	1.07	21.45	1.02	27.18	0.802
PA2 (Bernardo et al. 2013)	35.00	0.65	19.22	1.52	23.41	1.25	37.72	0.78	47.79	0.613
PA3 (Bernardo et al. 2013)	38.33	0.65	19.18	1.77	21.26	1.60	52.17	0.65	46.65	0.729
PA4 (Bernardo et al. 2013)	43.65	0.60	19.27	1.94	21.32	1.75	71.68	0.52	47.09	0.794
PB1 (Bernardo et al. 2013)	28.70	0.57	17.01	1.31	23.05	0.96	20.01	1.11	25.36	0.876
PB2 (Bernardo et al. 2013)	32.33	0.58	16.54	1.66	25.84	1.06	34.95	0.79	42.12	0.653
PB3 (Bernardo et al. 2013)	36.41	0.60	17.30	1.88	24.10	1.35	47.06	0.69	43.91	0.742
PB4 (Bernardo et al. 2013)	41.30	0.58	17.30	2.17	23.82	1.58	67.25	0.56	43.91	0.856
PC1 (Bernardo et al. 2013)	25.83	0.54	14.73	1.34	22.10	0.89	17.33	1.14	21.96	0.897
PC2 (Bernardo et al. 2013)	29.87	0.58	13.93	2.05	25.67	1.11	30.12	0.95	35.21	0.812
PC3 (Bernardo et al. 2013)	32.72	0.57	14.13	2.32	23.09	1.42	41.22	0.80	34.17	0.960
PC4 (Bernardo et al. 2013)	37.40	0.58	14.27	2.71	23.33	1.66	57.54	0.67	34.83	1.111
H3AR (Jeng 2015)	47.48	0.48	43.09	0.78	33.03	1.02	50.69	0.66	64.23	0.525
H2A (Jeng 2015)	51.12	0.30	51.86	0.69	33.45	1.07	61.00	0.59	77.29	0.463
H1AR (Jeng 2015)	48.96	0.65	55.28	0.69	29.72	1.29	65.03	0.59	82.39	0.466
H3B (Jeng 2015)	37.37	0.55	24.04	1.10	32.13	0.82	28.28	0.93	35.84	0.737
H2B (Jeng 2015)	41.14	0.66	27.06	1.09	31.83	0.93	31.83	0.93	40.33	0.732
H1B (Jeng 2015)	42.42	0.70	29.95	1.05	27.45	1.14	35.23	0.89	44.64	0.701
M3A (Jeng 2015)	39.85	0.49	43.09	0.70	27.75	1.08	50.69	0.59	57.79	0.519
M2A (Jeng 2015)	41.60	0.65	49.19	0.65	27.08	1.18	57.86	0.55	64.37	0.496
M1A (Jeng 2015)	44.96	0.70	55.27	0.64	25.13	1.41	65.02	0.54	72.52	0.488
M3B (Jeng 2015)	31.94	0.57	24.05	1.03	26.98	0.92	28.28	0.87	35.84	0.689
M2B (Jeng 2015)	34.11	0.77	27.06	0.97	26.08	1.00	31.83	0.82	40.33	0.650
M1B (Jeng 2015)	36.07	0.74	29.95	0.96	23.88	1.21	35.23	0.82	44.64	0.647
	$\bar{x}=0.59$		$\bar{x}=1.17$		$\bar{x}=1.13$		$\bar{x}=0.77$		$\bar{x}=0.68$	
	$s=0.12$		$s=0.63$		$s=0.22$		$s=0.18$		$s=0.19$	
	$cv=20\%$		$cv=54\%$		$cv=20\%$		$cv=23\%$		$cv=28\%$	

none of the studied codes of practice present equations. Table 5 also presents the ratios $M_{Tcr,\exp}/M_{Tcr,n}$ and $M_{Tu,\exp}/M_{Tu,n}$, as well as the corresponding and same statistical parameters presented in Table 4.

When compared with Table 4, the results from Table 5 show that the extended GSVATM fo PC beams provides much better estimates for the cracking torque when compared with ACI 318R-14 (ACI Committee 318 2014), and with lower dispersion of the results. The cracking torques from the ACI code are overestimated. For the ultimate (maximum torque), both ACI 318R-14 (ACI Committee 318 2014) and MC 10 (CEB-FIP MODEL 2010) codes slightly underestimate this important parameter for design, with higher dispersion of the results (mainly for the ACI code). Both EC 2 (NP EN 1992-1-1 1992) and CAN3-A23.3-14 (CSA Standard 2014) codes appreciably overestimate the ultimate torque, again with higher dispersion of the results. In general, it can be stated that the extended GSVATM for PC beams provides better estimates for the ultimate torque and with much lower dispersion of the results.

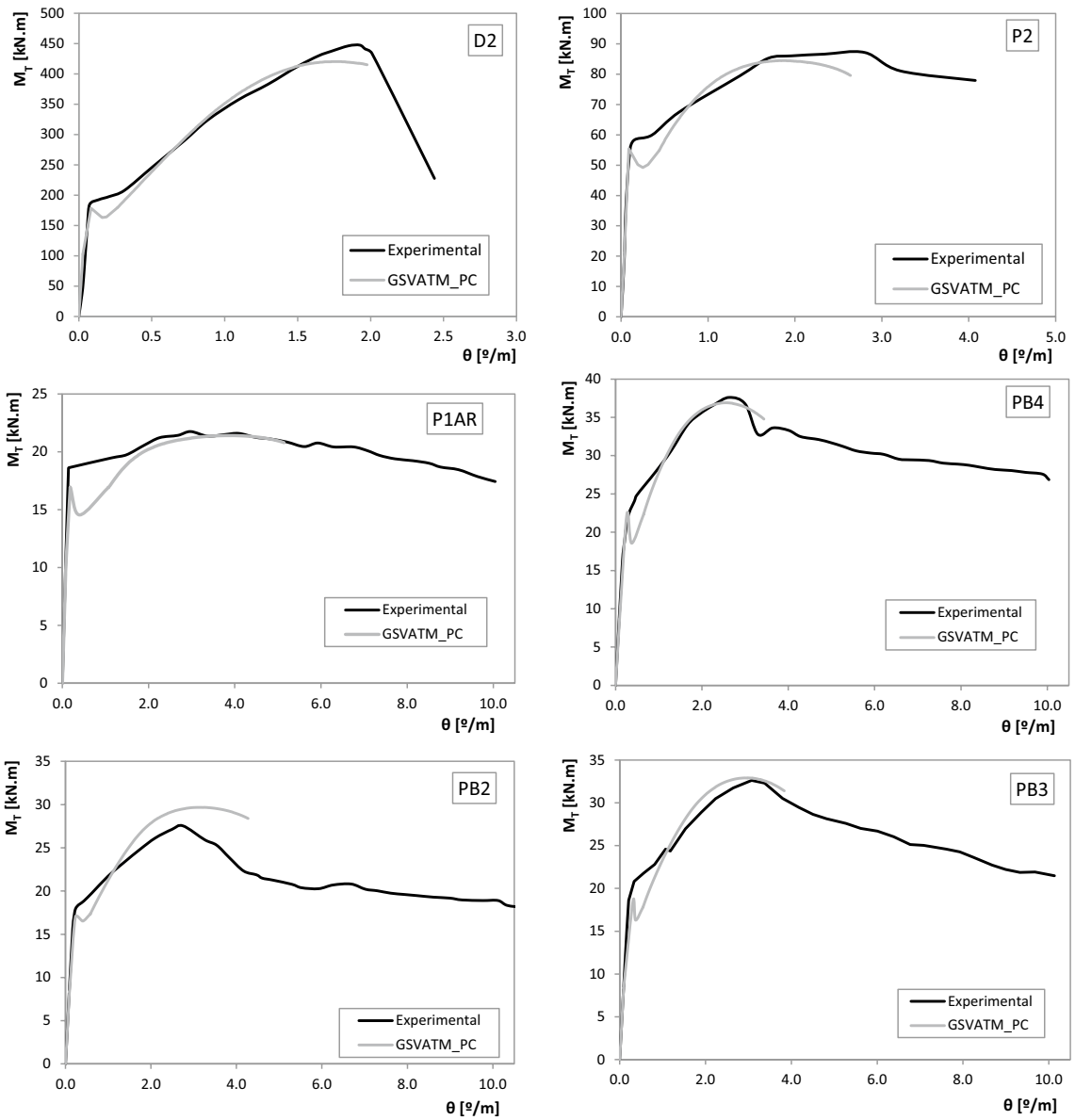

Fig. 2 $M_T-\theta$ curves for some reference PC beams.

5 Conclusions

In this study, the GSVATM previously proposed and validated for RC beams under torsion was extended in order to cover PC beams with longitudinal and uniform prestress, with both rectangular plain or hollow section. For this, the influence of prestressing was modelled in order to account for the initial stress state due to prestress. In addition, the contribution of the prestress reinforcement was accounted by incorporating into the GSVATM the contribution of the tensile σ–ε relationship of prestress steel. A new calculation procedure was presented to compute the solution points of the theoretical $M_T-\theta$ curves por PC beams, including for low loading stages.

Based on a comparative analysis with the experimental results of twenty-nine PC beams under torsion found in the literature, the following conclusions can be drawn:

- It was shown that the predictions from the GSVATM compare very well with the cracking torque and reasonably with the corresponding twist. In general, the transition from the non-cracked stage to the cracked stage is well predicted. These observations show that

the assumptions of GSVATM to model the influence of the initial stress state due to prestress are valid, despite pre-decompression concrete stage was not computed neither the influence of long term response was considered;

- It was also shown that the predictions from the GSVATM compare very well with the ultimate (resistance) torque and, again, reasonably with the corresponding twist. This observation shows that the assumptions of GSVATM to model the contribution of the prestress reinforcement for the torsional strength, namely the used tensile σ–ε relationship for prestress steel, are also valid;
- In addition, good agreement were also observed for the torsional stiffness, for the non-cracked stage and also the cracked stage for high loading levels.

In addition, when compared with the predictions of some codes of practice, namely for the cracking and ultimate torque, it was shown that the estimates from the GSVATM are in general more accurate.

The GSVATM extended for PC beams constitutes a contribution to generalize the Space-Truss Analogy for structural concrete members. This theoretical model can also be considered theoretically consistent because it is based on one single and generalized theory (VATM). Moreover, GSVATM can be used as a practical tool to help practitioners to optimize the design of PC beams under torsion.

Authors' contributions

CSBT and LFAB worked the theoretical model, developed the algorithms and analyzed the data. CSBT and JMAA developed the computing program to calculate the reference beams. LFAB and CSBT wrote the paper with the review by JMAA. All authors read and approved the final manuscript.

Author details

[1] C-MADE—Centre of Materials and Building Technologies, University of Beira Interior, Covilhã, Portugal. [2] University of Beira Interior, Covilhã, Portugal.

Competing Interests

The authors declare that they have no competing interests.

Publisher's Note

Received: 14 November 2017 Accepted: 26 June 2018
Published online: 03 October 2018

References

ACI Committee 318 (2014). Building Code Requirements for Reinforced Concrete (ACI 318-14) and Commentary (ACI 318R-14), American Concrete Institute, Detroit, MI.

Alnauimi, A. S., & Bhatt, P. (2004). Direct design of hollow reinforced concrete beams. Part I: design procedure. *Structural Concrete, 5*(4), 139–146.

Andrade, J. M. A., & Bernardo, L. F. A. (2013). Longitudinal/transversal prestressed hollow concrete beams under torsion: theoretical model and parametric analysis. In The 5th International Conference on THE CONCRETE FUTURE (CF13), 27–29 May, Covilhã, Portugal, CF51–CF59.

Ascione, L., Berardi, V. P., & D'Aponte, A. (2011). Long-term behavior of PC beams externally plated with prestressed FRP systems: a mechanical model. *Composites Part B Engineering, 42*(5), 1196–1201.

Bairan Garcia, J. M., & Mari Bernat, A. R. (2007). Shear-bending-torsion interaction in structural concrete members: A nonlinear coupled sectional approach. *Archives of Computational Methods in Engineering, 14*(3), 249–278.

Belarbi, A., & Hsu, T. C. (1994). Constitutive laws of concrete in tension and reinforcing bars stiffened by concrete. *Structural Journal of American Concrete Institute, 91*(4), 465–474.

Berardi, V. P., & Mancusi, G. (2012). Time-dependent behavior of reinforced polymer concrete columns under eccentric axial loading. *Materials, 5*(11), 2342–2352.

Berardi, V. P., & Mancusi, G. (2013). A mechanical model for predicting the long term behavior of reinforced polymer concretes. *Mechanics Research Communications, 50,* 1–7.

Bernardo, L. F. A., & Andrade, J. M. A. (2017). Prestressed concrete beams under torsion-extension of the VATM and evaluation of constitutive relationships. *Structural Engineering and Mechanics, 61*(5), 577–592.

Bernardo, L. F. A., Andrade, J. M. A., & Lopes, S. M. R. (2012a). Softened truss model for reinforced NSC and HSC beams under torsion: a comparative study. *Engineering Structures, 42,* 278–296.

Bernardo, L. F. A., Andrade, J. M. A., & Lopes, S. M. R. (2012b). Modified variable angle truss-model for torsion in reinforced concrete beams. *Materials and Structures, 45*(12), 1877–1902.

Bernardo, L. F. A., Andrade, J. M. A., & Nunes, N. C. G. (2015a). Generalized softened variable angle truss-model for reinforced concrete beams under torsion. *Materials and Structures, 48*(7), 2169–2193.

Bernardo, L. F. A., Andrade, J. M. A., & Oliveira, L. A. P. (2013). Reinforced and prestressed concrete hollow beams under torsion. *Journal of Civil Engineering and Management, 19*(S1), S141–S152.

Bernardo, L. F. A., & Lopes, S. M. R. (2008). Behaviour of concrete beams under torsion—NSC plain and hollow beams. *Materials and Structures, 41*(6), 1143–1167.

Bernardo, L. F. A., & Lopes, S. M. R. (2011). Theoretical behaviour of HSC sections under torsion. *Engineering Structures, 33*(12), 3702–3714.

Bernardo, L. F. A., Taborda, C. S. B., & Andrade, J. M. A. (2015b). Ultimate torsional behaviour of axially restrained RC beams. *Computers and Concrete, 16*(1), 67–97.

Bernardo, L. F. A., Taborda, C. S. B., & Gama, J. M. R. (2015c). Parametric analysis and torsion design charts for axially restrained RC beams. *Structural Engineering and Mechanics, 55*(1), 1–27.

Bhatti, M. A., & Almughrabi, A. (1996). Refined model to estimate torsional strength of reinforced concrete beams. *Journal of the American Concrete Institute, 93*(5), 614–622.

CEB-FIP MODEL CODE 2010, Comité Euro-International du Béton, Suisse.

CSA Standard. (2014). *Design of concrete structures—A23.3-14*. Mississauga: Canadian Standards Association.

El-Degwy, W. M., & McMullen, A. E. (1985). Prestressed concrete tests compared with torsion theories. *PCI Journal, 30,* 96–127.

Greene, G. G., & Belarbi, A. (2009). Model for RC members under torsion, bending, and shear. I: Theory. *Journal of Engineering Mechanics, 135*(9), 961–969.

Hsu, T. T. C. (1984). *Torsion of reinforced concrete*. New York: Van Nostrand Reinhold Company.

Hsu, T. T. C. (1993). *Unified theory of reinforced concrete*. Boca Raton: CRC Press.

Hsu, T. T. C., & Mo, Y. L. (1985a). Softening of concrete in torsional members—theory and tests. *Journal of the American Concrete Institute, 82*(3), 290–303.

Hsu, T. T. C., & Mo, Y. L. (1985b). Softening of concrete in torsional members—prestressed concrete. *Journal of the American Concrete Institute, 82*(5), 603–615.

Hsu, T. T. C., & Zhu, R. R. H. (2002). Softened membrane model for reinforced concrete elements in shear. *ACI Structural Journal, 99*(4), 460–469.

Jeng, C. H. (2015). Unified softened membrane model for torsion in hollow and solid reinforced concrete members modeling the entire precracking and postcracking behavior. *Journal of Structural Engineering, 141*(10), 04014243.

Jeng, C., Chiu, H., & Chen, C. (2010). Modeling the initial stresses in prestressed concrete members under torsion. *ASCE Conference Proceedings, 369*(162), 1773–1781.

Jeng, C.-H., & Hsu, T. T. C. (2009). A softened membrane model for torsion in reinforced concrete members. *Engineering Structures, 31,* 1944–1954.

Johnson, R. P. (1994). *Composite structures of steel and concrete*. Oxford: Blackwell Scientific Publications.
Karayannis, C. G. (2000). Smeared crack analysis for plain concrete in torsion. *Journal of Structural Engineering, 126*(6), 638–645.
Karayannis, C. G., & Chalioris, C. E. (2000). Experimental validation of smeared analysis for plain concrete in torsion. *Journal of Structural Engineering, 126*(6), 646–653.
Lopes, S. M. R., & Bernardo, L. F. A. (2014). Theoretical model for the mechanical behavior of prestressed beams under torsion. *Cogent Engineering, 1*(1), 943934.
Mitchell, D., & Collins, M. P. (1974). The behaviour of structural concrete in pure torsion civil engineering. Publication No. 74-06, Department of Civil Engineering, University of Toronto, March.
Nilson, A. H. (1987). *Design of prestressed concrete* (2nd ed.). Hoboken: Wiley.
Nobre, S. S. (2014). Modified variable angle truss model: Evaluation of the constitutive law for tensile concrete for the cracking of RC beams under torsion. Master Thesis. Department of Civil Engineering and Architecture, University of Beira Interior, Covilhã, Portugal **(in Portuguese)**.
NP EN 1992-1-1 (2010) Eurocode 2: Design of Concrete Structures—Part 1: General Rules and Rules for Buildings.
Price, A. M., & Anderson, D. (1992). *Composite beams in constructional steel design* (Vol. 4.1). Amsterdam: Elsevier Applied Science Publishers.
Rahal, K. N., & Collins, M. P. (1996). Simple model for predicting torsional strength of reinforced and prestressed concrete sections. *Journal of the American Concrete Institute, 93*(6), 658–666.
Rahal, K. N., & Collins, M. P. (2003). Combined torsion and bending in reinforced and prestressed concrete beams. *ACI Structural Journal, 100*(2), 157–165.
Rodrigues, J. A. T. F. (2011). Theoretical modelling of RC beams with longitudinal prestress under torsion with the SMMT. Master Thesis. Department of Civil Engineering and Architecture, University of Beira Interior, Covilhã, Portugal **(in Portuguese)**.
Silva, J. R. B., Horowitz, B., & Bernardo, L. F. A. (2017). Efficient procedure to analyze RC beam sections using the softened truss model. *ACI Structural Journal, 114*(3), 765–774.
Taborda, C. S. B. (2017). Generalization of the VATM and GSVATM to model structural concrete beams under torsion combined with uniforme axial stress state. PhD Thesis, Department of Civil Engineering and Architecture, Faculty of Engineering of University of Beira Interior, Covilhã, Portugal **(in Portuguese)**.
Vaz, A. N. S. (2014). Extension of the GSVATM to Reinforced Concrete Hollow Beams Under Torsion. Master Thesis. Department of Civil Engineering and Architecture, University of Beira Interior, Covilhã, Portugal **(in Portuguese)**.
Wafa, F. F., Shihata, S. A., Ashour, S. A., & Akhtaruzzaman, A. A. (1995). Prestressed high-strength concrete beams under torsion. *Journal of Structural Engineering, 121*(9), 1280–1286.
Wang, W., & Hsu, T. T. C. (1997). Limit analysis of reinforced concrete beams subjected to pure torsion. *Journal of Structural Engineering, 123*(1), 86–94.
Zhang, L. X., & Hsu, T. C. (1998). Behaviour and analysis of 100 MPa concrete membrane elements. *Journal of Structural Engineering, 124*(1), 24–34.